



## Original article

## Icariin enhances AMP-activated protein kinase and prevents high fructose and high salt-induced metabolic syndrome in rats

Abeer A. Aljehani<sup>a</sup>, Nawal A. Albadr<sup>a</sup>, Basma G. Eid<sup>b</sup>, Ashraf B. Abdel-Naim<sup>b,\*</sup><sup>a</sup> Department of Food Science and Nutrition, College of Food and Agriculture Sciences, King Saud University, Riyadh, Saudi Arabia<sup>b</sup> Department of Pharmacology and Toxicology, Faculty of Pharmacy, King Abdulaziz University, Jeddah, Saudi Arabia

## ARTICLE INFO

## Article history:

Received 23 May 2020

Accepted 27 August 2020

Available online 2 September 2020

## Keywords:

Metabolic syndrome

Icariin

AMPK

NFκB

## ABSTRACT

Metabolic syndrome (MetS) is an increasing health threat and often leads to cardiovascular complications. The aim of this study was to evaluate icariin's ability to combat MetS induced in rats and outline the involved mechanisms of action. Rats were grouped in four batches. The controls received a regular diet and water. MetS was induced in the remaining three groups using a high-salt high-fructose diet. Groups 1 and 2 were given daily doses of saline, while Groups 3 and 4 received 25 and 50 mg/kg icariin, respectively, for 12 weeks in total. The experimental protocol was carried out for 12 weeks consecutively. Icariin significantly decreased body mass index (BMI), adiposity index and body weight. Further, icariin protected against dyslipidemia, hyperglycemia, and hyperinsulinemia and improved insulin resistance as given by the homeostatic model assessment of insulin resistance (HOMA-IR) values. Icariin guarded against the rise in serum interleukin-6 (IL-6) and tumor necrosis factor alpha (TNF- $\alpha$ ). In addition, it significantly inhibited the decrease in mRNA expression of glucose transporter type 4 (GLUT4) and liver kinase B1 (LKB1). These effects were accompanied by decreased liver content of nuclear factor kappa B (NFκB) and enhanced serum levels of phosphorylated 5'-adenosine monophosphate-activated protein kinase (p-AMPK). Further, icariin significantly increased p-AMPK/AMPK ratio in liver tissues. Conclusively, icariin offers protection in experimentally induced MetS, partially due to AMPK activation.

© 2020 The Author(s). Published by Elsevier B.V. on behalf of King Saud University. This is an open access article under the CC BY-NC-ND license (<http://creativecommons.org/licenses/by-nc-nd/4.0/>).

## 1. Introduction

Metabolic syndrome (MetS) is a serious global health issue with a multifactorial nature and a rapidly expanding rate of incidence (Saklayen, 2018). It cannot be described as a specific disease because it is a combination of interconnected groups of different factors. These factors lead to the emergence of several clinical symptoms that potentiate risks of diabetes, cardiovascular disease, atherosclerosis, stroke, and all causes of death (Sherling et al., 2017). Insulin resistance, central obesity, glucose intolerance, high blood pressure, atherogenic dyslipidemia, and hypercoagulable state are considered different manifestations of MetS (Jaspinder,

2014). Several synthetic medicines have proven effective in reducing risk factors for metabolic syndrome (Koh et al., 2014). However, the current approach is to use natural herbs due to their safety, efficacy, and general approval by the scientific community and the public (Bauer, 2000). Many explanations have been proposed for the origin of MetS. Chronic low-grade inflammation, for example, is thought to be a main factor in MetS development and its associated pathological consequences (Sharma, 2011). In addition, activation of several metabolism pathways has been suggested as a preventive measure (McCracken et al., 2018). In particular, activation of 5'-adenosine monophosphate-activated protein kinase (AMPK) has been given attention (Ruderman et al., 2013). In this regard, LKB1 serves as an upstream kinase, which directly activates AMPK through phosphorylation. Therefore, the LKB1-AMPK pathway was proposed to possess a major regulatory role on metabolism (Shackelford & Shaw, 2009). As such, several AMPK activators have been demonstrated to reduce risks for the development of MetS and its related signs and symptoms (Ahn et al., 2008; Algardaby, 2020; Hwang et al., 2005).

Icariin is a flavanol glycoside obtained from the Epimedium variety and is utilized in conventional Chinese therapy (Lu et al., 2014). It offers several biologic and pharmacological activities,

\* Corresponding author at: Department of Pharmacology and Toxicology, Faculty of Pharmacy, King Abdulaziz University, Jeddah, Saudi Arabia.

E-mail address: [aaabdulrahman1@kau.edu.sa](mailto:aaabdulrahman1@kau.edu.sa) (A.B. Abdel-Naim).

Peer review under responsibility of King Saud University.



including antioxidant (Yang et al., 2020), cytotoxic (Alhakamy et al., 2020), phytoestrogenic (Xu et al., 2016), neuroprotective (Jia et al., 2019), osteoprotective (Pham et al., 2019), and anti-inflammatory (El-Shitany & Eid, 2019) effects. Experimentally, icariin has been shown to combat components of MetS as diabetes (Li et al., 2020), obesity (HAN et al., 2016), and dyslipidemia (Zhang et al., 2013). Further, studies have suggested that icariin enhances phosphorylation of 5' AMP-activated protein kinase (AMPK) (Han et al., 2015; Yunk-yung et al., 2016). Since it was suggested that AMPK activators could potentially treat and manage metabolic syndrome (Fryer & Carling, 2005; Sharma & Kumar, 2016), several natural products have been proposed to avert MetS. These include naringin, crocin, and green tea extract (Algandaby, 2020; Lukitasari et al., 2020; Pu et al., 2012). However, there are scarce data regarding the icariin's protection against metabolic syndrome. The current study aimed at evaluating the preventive roles of icariin against experimentally induced metabolic syndrome in a rat model.

## 2. Material and methods

### 2.1. Chemicals

Icariin > 98% from natural horny goat weed extract (Xi'an Nate Biological Technology Co., Ltd), China. Remaining chemicals had a purity of (>98%).

### 2.2. Animals and grouping

Thirty-two male Wistar rats (200–250 g) were brought from our animal facility (Faculty of Pharmacy, King Abdul-Aziz University, Saudi Arabia). Animals were kept at  $23 \pm 2$  °C with 12 h dark–light cycles. Ethical approval was obtained from the Research Ethics Committee at the Faculty of Pharmacy, King Abdulaziz University (Ref. PH-114-40). Rats were placed into four groups (eight rats each).

### 2.3. Animal treatment

Animals in Group 1 (control) were fed regular food pellets and water. MetS was induced in rats in Groups 2, 3, and 4 by providing them food pellets enriched with 3% sodium chloride and water with 10% fructose for 12 consecutive weeks (Abdallah et al., 2016; El-bassossy et al., 2016). At the eighth-week mark, animals in Groups 3 & 4 were given 25 or mg/kg icariin, respectively, by daily gavage until the end of week 12. Icariin treatments continued for five days per week until the end of the twelfth week. Doses were selected according to a pilot study and in line with doses used in previous investigations (Ding et al., 2017; Liu et al., 2018; Luo et al., 2007). Animal weights were recorded every four weeks. Upon completion of the twelfth week, animal lengths were recorded. Body mass index (BMI) was calculated as:

$$\text{BMI} = \text{body weight (g)} / \text{length}^2 (\text{cm}^2)$$

Blood glucose levels were obtained from tail vein blood samples after the twelfth week. At the beginning of the thirteenth week, blood was obtained from the retro-orbital plexus after placing the animals on light ether anesthesia. After coagulation of the blood samples, the samples were centrifuged to collect sera and kept at  $-80$  °C for subsequent biochemical analyses. Animals were sacrificed by decapitation under light ether anesthesia, and livers were rapidly harvested, cleaned, and kept at  $-80$  °C for further analyses. Visceral fat was collected from the abdomen of each rat and weighed. Adiposity index was calculated as follows (Bernardis, 1970):

$$\text{Adiposity index} = \sqrt[3]{\frac{\text{body weight (g)}}{\text{nose – to – anus length (cm)}}$$

### 2.4. Blood analysis

A glucometer (ACCU-CHEK, Roche, Mannheim, Germany) was employed for measuring fasting and postprandial glucose levels from tail vein blood. A rat insulin ELISA Kit (Catalog # MBS045315, MyBioSource, San Diego, USA) was employed for assaying fasting blood insulin in  $\mu\text{U/L}$ . Homeostatic model assessment of insulin resistance (HOMA-IR) was computed according (Harati et al., 2003) to

$$\text{HOMA – IR} = \frac{\text{Fasting glucose (mg/dL)} \times \text{Fasting insulin (mU/L)}}{405}$$

High-density lipoprotein cholesterol (HDL-C), low-density lipoprotein cholesterol (LDL-C), triglycerides (TG), total cholesterol (TC), and total protein were determined using commercially available kits (Catalog # CS606, CS607, CS611, CS603, and CS610, respectively), obtained from Crescent Diagnostics, Jeddah, Saudi Arabia.

### 2.5. Determination of serum pAMPK

An ELISA kit (Catalog # MBS7230575, MyBioSource, San Diego, USA) was used in assaying serum (phospho-5' AMP-activated protein kinase) pAMPK. Collected blood samples were left to coagulate at room temperature for 2 h. Then sera were obtained by centrifugation at 1000 g then stored at  $-80$  °C. The method employed a polyclonal anti-pAMPK antibody and an pAMPK-HRP conjugate and relied on competitive enzyme immunoassay technique. Incubation of the the assay sample and buffer with pAMPK-HRP conjugate took place for 1 h in a pre-coated plate. Wells were decanted and washed five times after incubation. An HRP enzyme substrate was added to the wells. A blue complex formed as a result of the enzyme-substrate reaction. The solution turns yellow after the addition of a stop solution in order to stop the reaction. Color intensity was measured at 450 nm spectrophotometrically. This intensity is inversely proportional to the pAMPK.

### 2.6. Real-time polymerase chain reaction

RNeasy mini kit (Qiagen, UK) was used to obtain RNA from the excised livers. SuperScript III cDNA Synthesis System (Invitrogen, UK) was used for reverse transcription of the RNA to complementary DNA (cDNA) after normalization of the RNA in the samples to 2  $\mu\text{g}$ . A 20  $\mu\text{l}$  reaction mixture was used, and Gene Runner Software was used in the primer design. In order to avoid contaminating genomic DNA (gDNA), primers were made of sequences of differing exons with spanning and flanking of introns. Primers for glucose transporter type 4 (GLUT4), liver kinase B1 (LKB1), and  $\beta$ -actin are sequenced in Table 1. A 7500 fast real-time PCR system (Applied Biosystems) was employed to obtain the expression patterns of the tested genes. A sample of 1  $\mu\text{l}$  synthesized cDNA (10 ng/ $\mu\text{l}$ ) was used as a template with 5  $\mu\text{l}$  PowerUp SYBR Green

**Table 1**  
Nucleotide sequences of the primers used for the analysis of mRNA expression by qRT-PCR.

Primer	Sequence (Forward / Reverse)
GLUT4	CCAGCAGATCCGCTCTGAAGA / AACATTGGAGTCATCAACGCC
LKB1	CCCGCGTCCGGGTGGAGTTTG / CCGCGACGGCCGACCGTCGCC
$\beta$ -actin	TGATAACCGGGAGATCGTGA / AAAGCACATCCAATAAAAAGC

PCR Master Mix and 0.75  $\mu$ l of the primers.  $\beta$ -actin was chosen as a housekeeping gene, and the tests were done in triplicate. A melt curve analysis was used for confirmation of qPCR reaction specificity. Results were validated by the relative quantification ( $\Delta\Delta$ Ct) method (Livak & Schmittgen, 2001). Mean value of  $\beta$ -actin was used to normalize the mean of the tested gene triplicates.

### 2.7. Preparation of liver homogenate

A glass Teflon homogenizer was used to homogenize approximately 0.5 g of tissues placed in 5 ml of ice-cooled phosphate buffer (0.1 M, pH 7.4 + 1% Triton x100). Homogenates were spun in a centrifuge at 4 °C and 4000  $\times$  g for twenty minutes. Nuclear extraction was performed on the collected supernatants.

### 2.8. Nuclear extract preparation

A EpiQuik™ nuclear extraction kit (OP-0002, Epigentek, NY, USA) was used for the preparation of nuclear extracts from liver samples. Levels of NF- $\kappa$ B were assessed using 100  $\mu$ g of the nuclear protein content.

### 2.9. NF- $\kappa$ B (p65) binding activity assessment

Abcam's NF- $\kappa$ B p65 Transcription Factor Assay Kit (ab133112) was used to determine NF- $\kappa$ B (p65) levels. This is dependent on the specific transcription factor DNA binding activity of the nuclear extracts. The technique also involved a 96-well ELISA. Next, immobilization of a specific double-stranded DNA (dsDNA) sequence with an NF- $\kappa$ B response element occurring in the wells, so that the nuclear extract NF- $\kappa$ B can specifically bind to the NF- $\kappa$ B response element. A primary antibody against the p65 subunit was used for NF- $\kappa$ B (p65) detection. A colorimetric recording at 450 nm was performed after addition of a secondary antibody conjugated to horseradish peroxidase (HRP). NF- $\kappa$ B (p65) levels are given relative to the control group (as a fold).

### 2.10. Protein expression of p-AMPK and AMPK by Western blot

RIPA lysis buffer (ice-cold) (ABCAM, Cambridge, MA, USA) containing protease and phosphatase inhibitor cocktails was employed to prepare liver tissue lysate; further, 100  $\mu$ g protein samples were added to every well of SDS-PAGE gel (concentration 10%). Separated proteins on gel were blotted onto a PVDF membrane (Bio-Rad Laboratories, Hercules, CA, USA) after electrophoresis. The membrane was sliced in half at a molecular weight of 55 kDa after blocking. Overnight incubation of the slice with proteins over 55 kDa was performed using the primary antibody rabbit polyclonal to AMPK (phospho S487) (catalog # ab131357) at a concentration of 1:500 (ABCAM, Cambridge, UK), followed by washing with 0.5% Tween-20 in TBS and incubation with HRP-

conjugated anti-rabbit secondary antibody (1:5000). An enhanced chemiluminescence (ECL) Western blotting kit (Licor®, NE, USA) was used to develop the membrane, and a Licor C-Digit Blot Scanner (Model 3600, NE, USA) was used for scanning. Then, the membrane was subjected to stripping and re-probed with the rabbit monoclonal (Y365) anti-AMPK (catalog # ab32047, ABCAM, Cambridge, UK). A rabbit monoclonal anti-GAPDH antibody (catalog # ab181602), ABCAM, Cambridge, UK) was used to probe the other membrane slice (<55 kDa). The relative band densities were quantified using ImageJ software version 1.46a (NIH, USA).

### 2.11. Statistical analysis

Findings are demonstrated as mean  $\pm$  SD. One-way analysis of variance (ANOVA), followed by a Tukey's post hoc test, was used to evaluate multiple comparisons. IBM SPSS® ver 25 (SPSS Inc., Chicago, IL, USA) was used for the analysis, where  $p < 0.05$  was considered significant.

## 3. Results

### 3.1. Effect of icariin on body weight gain and visceral fat

The data in Table 2 indicate that rats kept on high-fructose and high-salt food pellets in the experimental MetS group had significantly higher visceral fat accumulation, weight gain, and final body weights relative to controls. However, administration of icariin to rats significantly inhibited the weight gain dose-dependently. Interestingly, icariin at the higher dose (50 mg/kg) almost normalized visceral fat, body gain, and final body weight. When assessing final body length between all groups, no significant changes were noted. In addition, the MetS animals exhibited higher values of BMI when compared with control values (Fig. 1A). However, adiposity index was not significantly altered (Fig. 1B). The anti-obesity effects were confirmed by the significantly lower values of BMI and adiposity index in icariin-treated groups as compared with the MetS animals.

### 3.2. Effect of icariin on dyslipidemia induced by MetS

Animals in the MetS group showed a significant elevation of TG, TC, and LDL-C and decreased HDL-C relative to controls (Fig. 2 A, B, C, D). These effects of icariin on blood lipids were not related to the dose. Icariin at both dose levels did not cause increased TG and TC in comparison with the MetS group (Fig. 2A, B). In addition, values of serum LDL-C in icariin-treated groups were comparable with controls (Fig. 2C). However, the observed decline in HDL-C levels in MetS rats was not significantly modulated by administration of icariin (Fig. 2D).

**Table 2**

Effect of icariin on body weight gain and visceral fat in metabolic syndrome (MetS)-induced rats.

	Initial body weight (g)	Final body weight (g)	Weight gain (%)	Final body length (cm)	Visceral fat (g)
<b>Control</b>	205.5 $\pm$ 3.3	312.0 $\pm$ 14.8	51.9 $\pm$ 8.1	25.4 $\pm$ 1.3	10.3 $\pm$ 2.1
<b>MetS</b>	212.1 $\pm$ 8.5	430.7 <sup>a</sup> $\pm$ 23.8	103.3 <sup>a</sup> $\pm$ 12.8	24.8 $\pm$ 1.1	19.1 <sup>a</sup> $\pm$ 2.6
<b>MetS + icariin 25 mg/kg</b>	205.6 $\pm$ 5.3	385.0 <sup>a,b</sup> $\pm$ 22.5	87.1 <sup>a</sup> $\pm$ 8.1	28.9 $\pm$ 5.5	15.5 <sup>a,b</sup> $\pm$ 1.9
<b>MetS + icariin 50 mg/kg</b>	206.6 $\pm$ 3.4	332.2 <sup>b,c</sup> $\pm$ 18.3	60.2 <sup>b,c</sup> $\pm$ 7.5	30.3 $\pm$ 4.4	13.2 <sup>b</sup> $\pm$ 1.9

Data are presented as Mean  $\pm$  SD (n = 6).

Statistical analysis was performed by one-way ANOVA followed by Tukey test.

<sup>a</sup> Significant difference from control group at  $p < 0.05$ .

<sup>b</sup> Significant difference from MetS group at  $p < 0.05$ .

<sup>c</sup> Significant difference from icariin (25 mg/kg) group at  $p < 0.05$ .

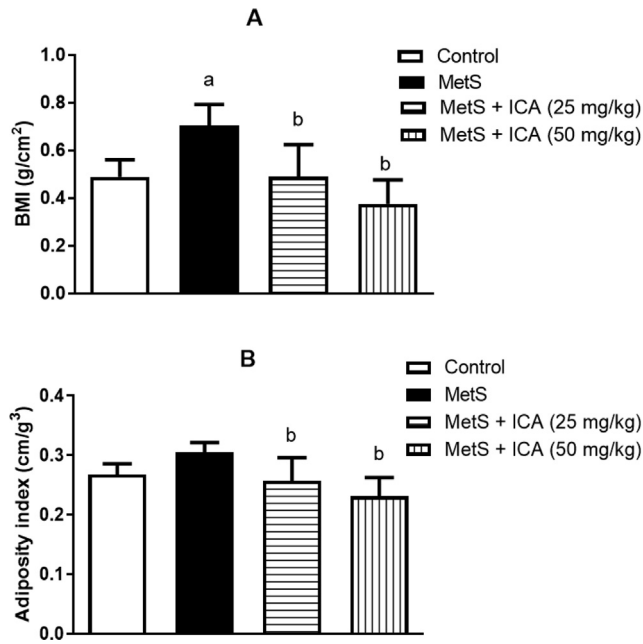


**Fig. 1.** Effect of icariin on body mass and adiposity indices in metabolic syndrome (MetS)-induced rats. Data are presented as Mean ± SD. a Significant difference from control group at  $p < 0.05$ . b Significant difference from MetS group at  $p < 0.05$ .

**3.3. Effect of icariin on fasting blood glucose, insulin concentrations, and HOMA-IR**

Keeping animals on a high-fructose and high-salt diet in the MetS group resulted in a significant rise in fasting glucose and insulin levels by 72% and 34%, respectively. Daily treatment of animals with icariin significantly ameliorated the rise in glucose and insulin levels. Insulin resistance as given by HOMA-IR was increased in MetS animals by 1.3-fold as compared with that of

the control animals. Icariin (25 and 50 mg/kg) mitigated the rise of HOMA-IR by 41% and 51%, respectively (Table 3).

**3.4. Effect of icariin on IL-6 and TNF- $\alpha$  in the serum**

Animals in the MetS syndrome showed significant elevation of IL-6 and TNF- $\alpha$  by 73% and 51% relative to control animals. Whereas, treatment of animals with icariin at 25 and 50 mg/kg successfully brought IL-6 and TNF- $\alpha$  levels to control values (Fig. 3A, B).

**4. Effect of icariin on mRNA expression of GLUT4 and LKB1 in the liver**

Induction of experimental MetS in animals was accompanied by downregulation of GLUT4 mRNA expression to almost half value of control rats. Icariin (25 and 50 mg/kg) significantly corrected this downregulation by 82% and 104% as compared with the MetS group (Fig. 4A). Similarly, the expression of LKB1 was significantly downregulated in the MetS animals by 66%. Icariin (25 and 50 mg/kg) alleviated inhibited expression of LKB1 to 70% and 84% of the control values, respectively (Fig. 4B).

**4.1. Effect of icariin on hepatic NF $\kappa$ b and pAMPK**

An 82% increase in liver content of NF $\kappa$ b (Fig. 5A) was observed after inducing MetS. However, icariin (25 and 50 mg/kg) mitigated the rise in NF $\kappa$ b by 27% and 32% respectively, relative to the MetS group. Further, MetS animals had significantly lower levels of pAMPK by 56% relative to the control animals. Nevertheless, oral gavage of rats with 25 or 50 mg/kg icariin inhibited the decrease in pAMPK levels. Icariin (50 mg/kg) brought the pAMPK content to almost control values (Fig. 5B).

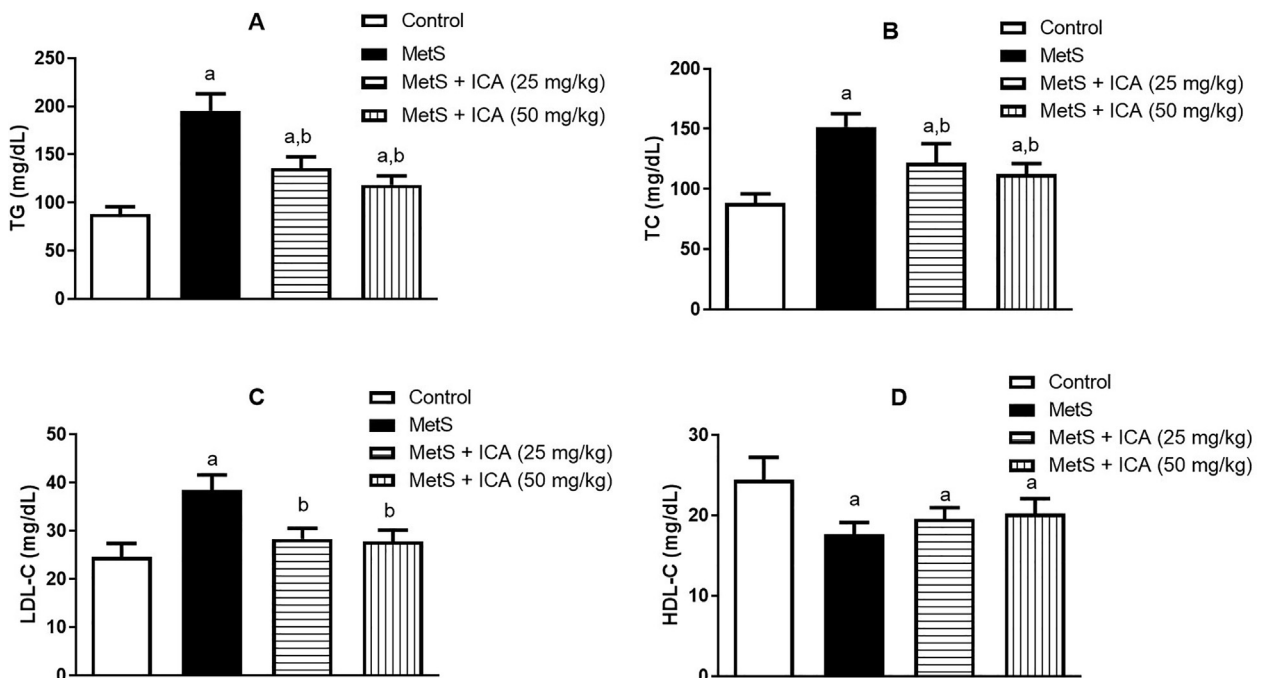


**Fig. 2.** Effect of icariin on blood lipids in metabolic syndrome (MetS)-induced rats. Data are presented as Mean ± SD. a Significant difference from control group at  $p < 0.05$ . b Significant difference from MetS group at  $p < 0.05$ .

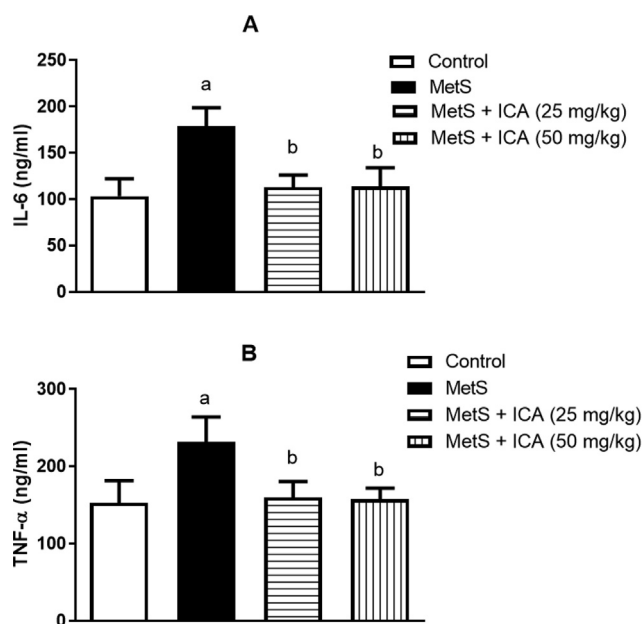
**Table 3**

Effect of icariin on fasting glucose and insulin levels and HOMA-IR in metabolic syndrome (MetS)-induced rats

	Fasting glucose (mmol/L)	Fasting insulin ( $\mu$ U/L)	HOMA-IR
Control	4.62 $\pm$ 0.41	12.15 $\pm$ 1.21	2.51 $\pm$ 0.46
MetS	7.98 <sup>a</sup> $\pm$ 0.63	16.34 <sup>a</sup> $\pm$ 1.13	5.79 <sup>a</sup> $\pm$ 0.59
MetS + icariin 25 mg/kg	6.14 <sup>a,b</sup> $\pm$ 0.77	12.42 <sup>b</sup> $\pm$ 1.07	3.39 <sup>a</sup> $\pm$ 0.55
MetS + icariin 50 mg/kg	5.18 <sup>b,c</sup> $\pm$ 0.53	12.22 <sup>b</sup> $\pm$ 0.96	2.81 <sup>b</sup> $\pm$ 0.25

Data are presented as Mean  $\pm$  SD (n = 6).

Statistical analysis was performed by one-way ANOVA followed by Tukey test.

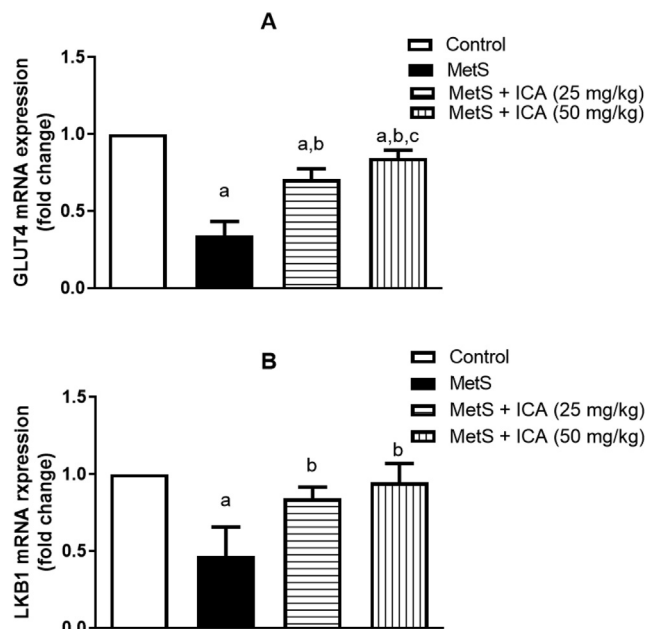
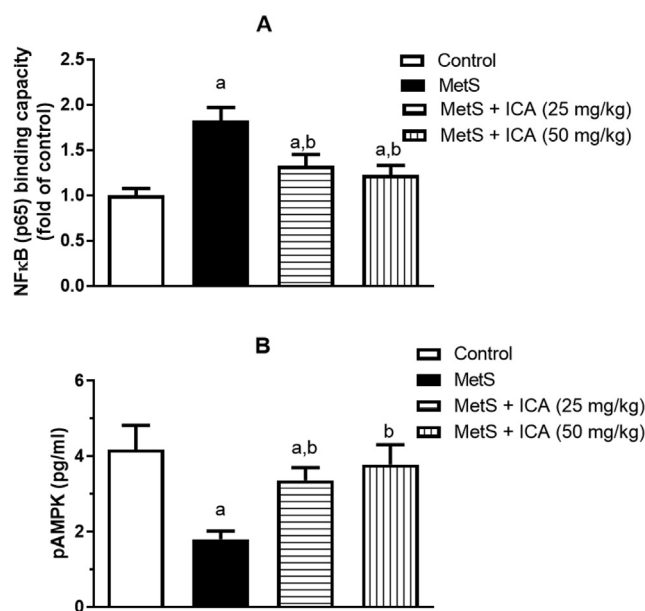
<sup>a</sup> Significant difference from control group at p < 0.05.<sup>b</sup> Significant difference from MetS group at p < 0.05.<sup>c</sup> Significant difference from icariin (25 mg/kg) group at p < 0.05.**Fig. 3.** Effect of icariin on serum IL-6 and TNF- $\alpha$  in metabolic syndrome (MetS)-induced rats. Data are presented as Mean  $\pm$  SD. a Significant difference from control group at p < 0.05. b Significant difference from MetS group at p < 0.05.

#### 4.2. Assessment of p-AMPK /AMPK ratio

The p-AMPK and total AMPK expression in liver tissue following icariin treatment (25 & 50 mg/kg orally) were investigated by Western blot (Fig. 6). The total protein expression of AMPK was observed and proved not significantly different. However, a marked decrease in p-AMPK expression was noted in the MetS group relative to control. Icariin at 25 mg/kg enhanced p-AMPK expression compared with MetS group, as shown by the significant increase in p-AMPK/total AMPK ratio by densitometric quantitation (Fig. 6). It is worth noting that icariin treatment with 50 mg/kg significantly increased this ratio as compared with all other groups.

### 5. Discussion

The present study aimed at evaluating the potential of icariin to prevent experimental MetS due to high-fructose food and high-salt intake in rats. Icariin at 25 and 50 mg/kg doses successfully inhibited weight gain, accumulation of visceral fat, and the rise in BMI and adiposity index. These findings gain support by a previous report highlighting the anti-adipogenic effects of icariin and its

**Fig. 4.** Effect of icariin on hepatic mRNA expression of GLUT4 and LKB1 in metabolic syndrome (MetS)-induced rats. Data are presented as Mean  $\pm$  SD. a Significant difference from control group at p < 0.05. b Significant difference from MetS group at p < 0.05. c Significant difference from icariin (25 mg/kg) group at p < 0.05.**Fig. 5.** Effect of icariin on serum pAMPK in metabolic syndrome (MetS)-induced rats. Data are presented as Mean  $\pm$  SD. a Significant difference from control group at p < 0.05. b Significant difference from MetS group at p < 0.05.

antiproliferative activity against adipocytes (HAN et al., 2016). Further, the structurally related compound anhydroicaritin has been reported to mitigate diet-induced obesity and hyperlipidemia in mice (Zheng et al., 2016). Furthermore, the current data showed that icariin exhibited anti-dyslipidemic effects. This is consistent with the reported ability of icariin to reduce serum lipid and fructose levels in streptozotocin-challenged rats (Gong et al., 2013). In addition, our findings are in line with the aptitude of icariin to decrease TC and LDL-C in high-cholesterol-fed rabbits. This lipid-lowering was attributed to upregulation of Lipe and Pnpla2, which

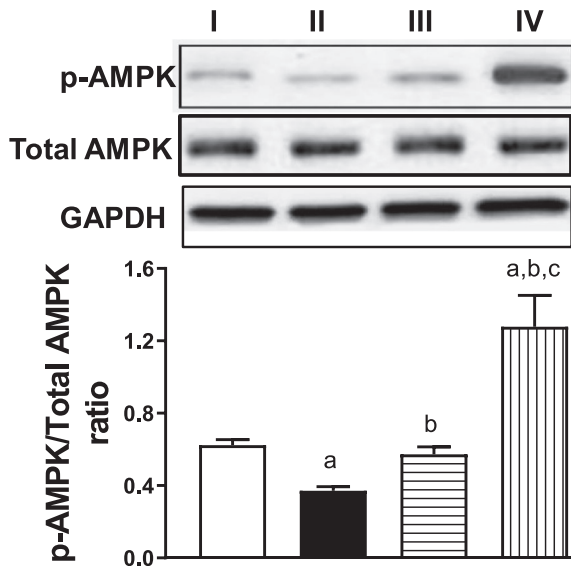


**Fig 6.** Effect of icariin on pAMPK protein expression in liver tissues. Data are presented as Mean  $\pm$  SD. a Significant difference from control group at  $p < 0.05$ . b Significant difference from MetS group at  $p < 0.05$ . c Significant difference from icariin (25 mg/kg) group at  $p < 0.05$ .

are genes that cause lysis of lipids in liver tissues (Zhang et al., 2013). This is in line with a report indicating the ability of icariin to up-regulate Lipe and Pnpla2 in mice liver tissues (Lu et al., 2014). However, no significant alterations were observed in HDL-C. Unlike humans, cholesterol is contained in HDL-C not LDL-C (Wang et al., 2010). Therefore, a longer duration of animal treatment may have been needed to show such effects on HDL-C. Hyperglycemia and insulin resistance are between the hallmarks of MetS (Srikanthan et al., 2016). Metabolic syndrome induced by fructose has been well studied, especially its ability to cause insulin resistance and de novo lipogenesis (Pan and Kong, 2018). In addition, continuous fructose intake induces liver synthesis of triose-phosphate, causing a surge in triglycerides and insulin resistance in the liver (Tappy, 2018). In the current investigation, keeping rats on high-fructose water resulted in elevation of fasting blood glucose, insulin, and HOMA-IR. Nevertheless, icariin guarded against the rise in both fasting glucose and insulin. Consequently, MetS-induced insulin resistance was improved, as shown by the observed decrease in HOMA-IR values in the treated rats. These observations are consistent with reported data demonstrating the anti-hyperglycemic activities of icariin in type 2 diabetic rats as well as protecting pancreatic functions (Li et al., 2020). Further, icariin protected against diabetic complications as bone loss (Qi et al., 2019), cardiomyopathy (Qiao et al., 2020), erectile dysfunction (Wang et al., 2017), nephropathy (Qi et al., 2011), and retinopathy (Xin et al., 2012). This is in addition to the reported improvement in insulin resistance in experimental type 2 diabetes by icariin (Qiao et al., 2020). *In vitro*, icariin has been shown to mitigate palmitate-induced insulin resistance via inhibiting thioredoxin-interacting protein (TXNIP) and decreasing endoplasmic reticulum stress in C2C12 mouse muscle cells (Li et al., 2018). Also, icariin activates the AMPK pathway in C2C12 cells and reduces insulin resistance (Han et al., 2015).

Several theories have elucidated the origin of MetS. Chronic low-grade inflammatory conditions, for example, have been implicated as a major factor of MetS and its associated pathophysiological consequences (De Ferranti & Mozaffarian, 2008). In addition, several studies support the concept that a proinflammatory state is a component of MetS (Sharma, 2011). This has been widely

accepted by the scientific community to the extent of considering MetS as an inflammatory disorder (Reddy et al., 2019). Our data are in line with these explanations, as MetS rats exhibited increased IL-6 and TNF- $\alpha$ . The suggested anti-MetS properties of icariin are supported by the significantly lower levels of these inflammatory markers. These results are further substantiated by the propensity of icariin derivatives to inhibit inflammation by suppressing p38 mitogen-activated protein kinase and NF- $\kappa$ B pathways (Shao-Rui et al., 2010). Icariin was also shown to modulate the HO-1/Nrf2 and NF- $\kappa$ B signaling pathways and prevent carrageenan-induced acute inflammation (El-Shitany & Eid, 2019). The role of fructose-induced inflammation in developing hyperlipidemia and insulin resistance has been reviewed (Bidwell, 2017). Thus, the observed anti-inflammatory activities of icariin lend explanation for icariin's ability to improve dyslipidemia and insulin resistance associated with MetS. Insulin stimulates glucose uptake into fat and muscles by activating GLUT4 (Klip et al., 2019). Therefore, disruption of GLUT4 has been linked to insulin resistance (Mueckler, 2001). Amelioration of GLUT4 downregulation has been shown to mediate prevention of insulin resistance by phytochemicals (Neisy et al., 2019). The observed ability of icariin to mitigate GLUT4 downregulation is in line with the literature (Li et al., 2020) in which icariin decreased sugar levels in type 2 diabetic rats via upregulation of GLUT4. Hence, icariin's positive impact on MetS-associated downregulation of GLUT4 further explains improvement of HOMA-IR values.

AMPK has been widely documented for its role in preventing MetS and diabetes (Kim et al., 2016). Further, insulin resistance and MetS were prevented by AMPK activators. In particular, numerous polyphenols have been shown to activate AMPK and exert favorable effects on diabetes and MetS. Examples include resveratrol (Baur et al., 2006), quercetin (Ahn et al., 2008), crocin (Algandaby, 2020), and epigallocatechin gallate (Hwang et al., 2005). Mechanisms of activation of AMPK by polyphenolic compounds involves elevation of AMP levels via inhibiting mitochondrial ATP production (Gledhill et al., 2007; Zheng & Ramirez, 2000). Most of these actions are related to phosphorylation at Thr172. However, phosphorylation at S487 mediates several physiological or pathological actions. Protein kinase A activation-induced insulin resistance is regulated by reduced AMPK activity via phosphorylates AMP-activated protein kinase  $\alpha$ 1 Ser487 (Heathcote et al., 2016). Further, phosphorylation by Akt within the ST loop of AMPK- $\alpha$ 1 down-regulates its activation in tumor cells (Heathcote et al., 2016). In this study, icariin significantly ameliorated downregulation of LKB1, which is a primary upstream of AMPK (Shackelford & Shaw, 2009). Also, icariin's ability to enhance p-AMPK gains support via several investigations (Chen et al., 2019; Han et al., 2016; Li et al., 2020). Thus, observed preservation of LKB1 expression and enhancement of serum phosphorylation of AMPK by icariin are homogenous and provide a strong basis for explaining its anti-MetS activities. Elevated active AMPK in the blood can help to explain the observed icariin pharmacological activities. In brief, activated AMPK inhibits several anabolic pathways including lipid and sterol synthesis. This involves inhibition of phosphorylation of the acetyl-CoA carboxylases ACC1 and ACC2, which catalyze de novo lipid synthesis. In addition, activated AMPK blocks gluconeogenesis by CRTC2 phosphorylation (Koo et al., 2005). Actually, AMPK has significant impact on key regulators of transcription of glucose and lipid metabolism. It enhances phosphorylation of sterol regulatory element-binding protein 1 (SREBP1) (Li et al., 2011), carbohydrate-responsive element binding protein (ChREBP) (Kawaguchi et al., 2002) and hepatocyte nuclear factor 4 $\alpha$  (HNF4 $\alpha$ ) (Hong et al., 2003). These data give explanations for the observed anti-dyslipidemic and anti-hyperglycemic effects of icariin. The exact source and half-life time of blood p-AMPK is unknown. However, it has distinct endocrine

actions that participate in energy preservation. In addition to its anti-anabolic actions, active AMPK, stimulates several catabolic pathways. AMPK enhances glucose consumption by phosphorylating TXNIP13 and TBC1D1 (Chavez et al., 2008) and increasing the localization of GLUT1 and GLUT4 in the plasma membrane respectively. Glucose uptake is also indirectly augmented by AMPK-mediated phospholipase D1 (PLD1) phosphorylation (Kim et al., 2010). Further, exhaustion of lipid stores is accelerated by the enzymatic activity of pAMPK. This can be attributed to ability of the enzyme to indirectly decrease malonyl CoA, resulting in enhanced mitochondrial fatty acids  $\beta$ -oxidation and decreased lipid synthesis (Herzig and Shaw, 2018). So, the observed antihyperlipidemic activities of icariin can be explained on the ability of pAMPK to inhibit fatty acid synthase, HMG-CoA reductase and hormone-sensitive lipase. These result in less synthesis of cholesterol and fatty acids, oxidation and lipolysis (Kahn et al., 2005; Kola et al., 2006). Finally, activated AMPK is known to block the inflammation and signaling of NF- $\kappa$ B (Salminen et al., 2011). This complies with the observed inhibition of NF- $\kappa$ B in liver tissues and supports the anti-inflammatory effects of icariin, which indicates that icariin possesses a plethora of pharmacological actions.

## 6. Conclusion

In this study, the preventive effects of icariin against MetS resulting from high-fructose high-salt diets were evaluated in rats. Icariin ameliorated signs of MetS, as evidenced by preventing the rise in weight gain, visceral fat accumulation, body mass and adiposity indices, dyslipidemia, hyperglycemia, and hyperinsulinemia. This was accompanied by preventing increased serum IL-6 and TNF- $\alpha$  and upregulating mRNA expression of GLUT4 and LKB1. Further, icariin significantly increased serum levels of p-AMPK and p-AMPK/AMPK ratio in hepatic tissues. Thus, these observed beneficial effects of icariin can be attributed, at least partly, to enhancement of serum level and liver content of p-AMPK.

## Declaration of Competing Interest

The authors declare that they have no known competing financial interests or personal relationships that could have appeared to influence the work reported in this paper.

## Acknowledgement

The authors would like to thank Deanship of Scientific Research in King Saud University for funding and supporting this research through the initiative of DSR Graduate Students Research Support (GSR).

## References

Abdallah, H.M., El-Bassossy, H.M., Mohamed, G.A., El-Halawany, A.M., Alshali, K.Z., Banjar, Z.M., 2016. Phenolics from *Garcinia mangostana* alleviate exaggerated vasoconstriction in metabolic syndrome through direct vasodilatation and nitric oxide generation. *BMC Complement. Altern. Med.* 16, 359. <https://doi.org/10.1186/s12906-016-1340-5>.

Ahn, J., Lee, H., Kim, S., Park, J., Ha, T., 2008. The anti-obesity effect of quercetin is mediated by the AMPK and MAPK signaling pathways. *Biochem. Biophys. Res. Commun.* 373, 545–549. <https://doi.org/10.1016/j.bbrc.2008.06.077>.

Algandaby, M.M., 2020. Crocin prevents metabolic syndrome in rats via enhancing PPAR-gamma and AMPK. *Saudi J. Biol. Sci.* <https://doi.org/10.1016/j.sjbs.2020.01.004>.

Alhakamy, N.A., Fahmy, U.A., Badr-Eldin, S.M., Ahmed, O.A.A., Asfour, H.Z., Aldawsari, H.M., Algandaby, M.M., Eid, B.G., Abdel-Naim, A.B., Awan, Z.A., Alruwaili, N.K., Mohamed, A.I., 2020. Optimized icariin phytosomes exhibit enhanced cytotoxicity and apoptosis-inducing activities in ovarian cancer cells. *Pharmaceutics* 12. <https://doi.org/10.3390/pharmaceutics12040346>.

Bauer, B.A., 2000. Herbal therapy: What a clinician needs to know to counsel patients effectively. *Mayo Clin. Proc.* <https://doi.org/10.4065/75.8.835>.

Baur, J.A., Pearson, K.J., Price, N.L., Jamieson, H.A., Lerin, C., Kalra, A., Prabhu, V.V., Allard, J.S., Lopez-Lluch, G., Lewis, K., Pistell, P.J., Poosala, S., Becker, K.G., Boss, O., Gwinn, D., Wang, M., Ramaswamy, S., Fishbein, K.W., Spencer, R.G., Lakatta, E.G., Le Couteur, D., Shaw, R.J., Navas, P., Puigserver, P., Ingram, D.K., De Cabo, R., Sinclair, D.A., 2006. Resveratrol improves health and survival of mice on a high-calorie diet. *Nature* 444, 337–342. <https://doi.org/10.1038/nature05354>.

Bernardis, L.L., 1970. Prediction of carcass fat, water and lean body mass from Lee's 'nutritive ratio' in rats with hypothalamic obesity. *Experientia* 26, 789–790. <https://doi.org/10.1007/BF02232553>.

Bidwell, A.J., 2017. Chronic fructose ingestion as a major health concern: Is a sedentary lifestyle making it worse? A review. *Nutrients*. <https://doi.org/10.3390/nu9060549>.

Chavez, J.A., Roach, W.G., Keller, S.R., Lane, W.S., Lienhard, G.E., 2008. Inhibition of GLUT4 translocation by Tbc1d1, a Rab GTPase-activating protein abundant in skeletal muscle, is partially relieved by AMP-activated protein kinase activation. *J. Biol. Chem.* 283, 9187–9195. <https://doi.org/10.1074/jbc.M708934200>.

Chen, S.Q., Ding, L.N., Zeng, N.X., Liu, H.M., Zheng, S.H., Xu, J.W., Li, R.M., 2019. Icariin induces irisin/FNDC5 expression in C2C12 cells via the AMPK pathway. *Biomed. Pharmacother.* 115. <https://doi.org/10.1016/j.biopha.2019.108930>.

De Ferranti, S., Mozaffarian, D., 2008. The perfect storm: Obesity, adipocyte dysfunction, and metabolic consequences. *Clin. Chem.* <https://doi.org/10.1373/clinchem.2007.100156>.

Ding, J., Tang, Y.T.Z., Qi, X.Z.L., Wang, X.Z.G., 2017. Icariin improves the sexual function of male mice through the PI3K / AKT / eNOS / NO signalling pathway 1–6. <https://doi.org/10.1111/and.12802>.

El-bassossy, H.M., Elberry, A.A., Ghareib, S.A., 2016. Journal of Diabetes and Its Complications Geraniol improves the impaired vascular reactivity in diabetes and metabolic syndrome through calcium channel blocking effect. *J. Diabetes Complications* 30, 1008–1016. <https://doi.org/10.1016/j.jdiacomp.2016.04.006>.

El-Shitany, N.A., Eid, B.G., 2019. Icariin modulates carrageenan-induced acute inflammation through HO-1/Nrf2 and NF- $\kappa$ B signaling pathways. *Biomed. Pharmacother.* 120. <https://doi.org/10.1016/j.biopha.2019.109567>.

Fryer, L.G.D., Carling, D., 2005. AMP-activated protein kinase and the metabolic syndrome, in: *Biochemical Society Transactions*. Biochem Soc Trans, pp. 362–366. <https://doi.org/10.1042/BST0330362>.

Gledhill, J.R., Montgomery, M.G., Leslie, A.G.W., Walker, J.E., 2007. Mechanism of inhibition of bovine F1-ATPase by resveratrol and related polyphenols. *Proc. Natl. Acad. Sci. U.S.A.* 104, 13632–13637. <https://doi.org/10.1073/pnas.0706290104>.

Gong, Y., Shi, J., Xie, G., Liu, H., Qi, M., 2013. Amelioration of icariin for the epididymis impairment induced by streptozocin (STZ) in rats. *Zhongguo Ying Yong Sheng Li Xue Za Zhi*. 29, 47–50.

Han, Y., Jung, H.W., Park, Y.K., 2015. Effects of Icariin on insulin resistance via the activation of AMPK pathway in C2C12 mouse muscle cells. *Eur. J. Pharmacol.* 758, 60–63. <https://doi.org/10.1016/j.ejphar.2015.03.059>.

Han, Y.Y., Song, M.Y., Hwang, M.S., Hwang, J.H., Park, Y.K., Jung, H.W., 2016. Epimedium koreanum Nakai and its main constituent icariin suppress lipid accumulation during adipocyte differentiation of 3T3-L1 preadipocytes. *Chin. J. Nat. Med.* 14, 671–676. [https://doi.org/10.1016/S1875-5364\(16\)30079-6](https://doi.org/10.1016/S1875-5364(16)30079-6).

Harati, M., ANI, A., MESRIPOUR, M., 2003. Effect of vanadyl sulfate on fructose-induced insulin resistance rat.

Heathcote, H.R., Mancini, S.J., Strembitska, A., Jamal, K., Reihill, J.A., Palmer, T.M., Gould, G.W., Salt, I.P., 2016. Protein kinase C phosphorylates AMP-Activated protein kinase  $\alpha$ 1 Ser487. *Biochem. J.* 473, 4681–4697. <https://doi.org/10.1042/BCJ20160211>.

Herzig, S., Shaw, R.J., 2018. AMPK: Guardian of metabolism and mitochondrial homeostasis. *Nat. Rev. Mol. Cell Biol.* <https://doi.org/10.1038/nrm.2017.95>.

Hong, Y.H., Varanasi, U.S., Yang, W., Leff, T., 2003. AMP-activated protein kinase regulates HNF4 $\alpha$  transcriptional activity by inhibiting dimer formation and decreasing protein stability. *J. Biol. Chem.* 278, 27495–27501. <https://doi.org/10.1074/jbc.M304112200>.

Hwang, J.T., Park, I.J., Shin, J.I., Lee, Y.K., Lee, S.K., Baik, H.W., Ha, J., Park, O.J., 2005. Genistein, EGCG, and capsaicin inhibit adipocyte differentiation process via activating AMP-activated protein kinase. *Biochem. Biophys. Res. Commun.* 338, 694–699. <https://doi.org/10.1016/j.bbrc.2005.09.195>.

Jaspinder, K., 2014. A comprehensive review on metabolic syndrome. *Cardiol. Res. Pract.* 2014. <https://doi.org/10.1155/2014/943162>.

Jia, G., Zhang, Y., Li, W., Dai, H., 2019. Neuroprotective role of icariin in experimental spinal cord injury via its antioxidant, anti-neuroinflammatory and anti-apoptotic properties. *Mol. Med. Rep.* 20, 3433–3439. <https://doi.org/10.3892/mmr.2019.10537>.

Kahn, B.B., Alquier, T., Carling, D., Hardie, D.G., 2005. AMP-activated protein kinase: Ancient energy gauge provides clues to modern understanding of metabolism. *Cell Metab.* <https://doi.org/10.1016/j.cmet.2004.12.003>.

Kawaguchi, T., Osatomi, K., Yamashita, H., Kabashima, T., Uyeda, K., 2002. Mechanism for fatty acid “sparing” effect on glucose-induced transcription: Regulation of carbohydrate-responsive element-binding protein by AMP-activated protein kinase. *J. Biol. Chem.* 277, 3829–3835. <https://doi.org/10.1074/jbc.M107895200>.

Kim, J.H., Park, J.M., Yea, K., Kim, H.W., Suh, P.G., Ryu, S.H., 2010. Phospholipase D1 mediates AMP-activated protein kinase signaling for glucose uptake. *PLoS ONE* 5. <https://doi.org/10.1371/journal.pone.0009600>.

Kim, Jongmok, Yang, G., Kim, Y., Kim, J.H., 2016. REVIEW AMPK activators: mechanisms of action and physiological activities 1–12. <https://doi.org/10.1038/emm.2016.16>.

- Klip, A., McGraw, T.E., James, D.E., 2019. Thirty sweet years of GLUT4. *J. Biol. Chem.* <https://doi.org/10.1074/jbc.REV119.008351>.
- Koh, S., Kim, J.M., Kim, I., Ko, S.H., Kim, J.S., 2014. Anti-inflammatory mechanism of metformin and its effects in intestinal inflammation and colitis-associated colon cancer. *Anti-inflammatory mechanism of metformin and its effects in intestinal inflammation and colitis-associated colon 1*. <https://doi.org/10.1111/jgh.12435>.
- Kola, B., Boscaro, M., Rutter, G.A., Grossman, A.B., Korbonits, M., 2006. Expanding role of AMPK in endocrinology. *Trends Endocrinol Metab.* <https://doi.org/10.1016/j.tem.2006.05.006>.
- Koo, S.H., Flechner, L., Qi, L., Zhang, X., Sreter, R.A., Jeffries, S., Hedrick, S., Xu, W., Boussouar, F., Brindle, P., Takemori, H., Montminy, M., 2005. The CREB coactivator TORC2 is a key regulator of fasting glucose metabolism. *Nature* 437, 1109–1114. <https://doi.org/10.1038/nature03967>.
- Li, M., Zhang, Y., Cao, Y., Zhang, D., Liu, L., Guo, Y., Wang, C., 2018. Icaritin ameliorates palmitate-induced insulin resistance through reducing thioredoxin-interacting protein (TXNIP) and suppressing ER stress in C2C12 myotubes. *Front. Pharmacol.* 9, 1–12. <https://doi.org/10.3389/fphar.2018.01180>.
- Li, X., Wang, Y., Shi, P., Liu, Y., Li, T., Liu, S., Wang, C., Wang, L., Cao, Y., 2020. Icaritin treatment reduces blood glucose levels in type 2 diabetic rats and protects pancreatic function. *Exp. Ther. Med.* 19, 2690–2696. <https://doi.org/10.3892/etm.2020.8490>.
- Li, Y., Xu, S., Mihaylova, M.M., Zheng, B., Hou, X., Jiang, B., Park, O., Luo, Z., Lefai, E., Shyy, J.Y.J., Gao, B., Wierzbicki, M., Verbeuren, T.J., Shaw, R.J., Cohen, R.A., Zang, M., 2011. AMPK phosphorylates and inhibits SREBP activity to attenuate hepatic steatosis and atherosclerosis in diet-induced insulin-resistant mice. *Cell Metab.* 13, 376–388. <https://doi.org/10.1016/j.cmet.2011.03.009>.
- Liu, J., Mattheos, N., Su, C., Deng, C., Luo, N., Wang, Z., Tang, H., 2018. The effects of icaritin on wound healing of extraction sites with administration of zoledronic acid and dexamethasone: A rat model study 198–205. <https://doi.org/10.1111/jop.12659>.
- Livak, K.J., Schmittgen, T.D., 2001. Analysis of relative gene expression data using real-time quantitative PCR and the 2- $\Delta\Delta$ CT method. *Methods* 25, 402–408. <https://doi.org/10.1006/meth.2001.1262>.
- Lu, Y.F., Xu, Y.Y., Jin, F., Wu, Q., Shi, J.S., Liu, J., 2014. Icaritin is a PPAR $\alpha$  activator inducing lipid metabolic gene expression in mice. *Molecules* 19, 18179–18191. <https://doi.org/10.3390/molecules191118179>.
- Lukitasari, M., Nugroho, D., Rohman, M., Widodo, N., Farmawati, A., Hastuti, P., 2020. Beneficial effects of green coffee and green tea extract combination on metabolic syndrome improvement by affecting AMPK and PPAR- $\alpha$  gene expression. *J. Adv. Pharm. Technol. Res.* 11, 81–85. [https://doi.org/10.4103/japtr.JAPTR\\_116\\_19](https://doi.org/10.4103/japtr.JAPTR_116_19).
- Luo, Y., Nie, J., Gong, Q., Lu, Y., Wu, Q., Shi, J., 2007. Protective effects of icaritin against learning and memory deficits induced by aluminium in rats. 792–795. <https://doi.org/10.1111/j.1440-1681.2007.04647.x>.
- McCracken, E., Monaghan, M., Sreenivasan, S., 2018. Pathophysiology of the metabolic syndrome. *Clin. Dermatol.* 36, 14–20. <https://doi.org/10.1016/j.clindermatol.2017.09.004>.
- Mueckler, M., 2001. Insulin resistance and the disruption of GLUT4 trafficking in skeletal muscle. *J. Clin. Invest.* <https://doi.org/10.1172/JCI13020>.
- Neisy, A., Zal, F., Seghatoleslam, A., Alaei, S., 2019. Amelioration by quercetin of insulin resistance and uterine GLUT4 and ER $\alpha$  gene expression in rats with polycystic ovary syndrome (PCOS). *Reprod. Fertil. Dev.* 31, 315–323. <https://doi.org/10.1071/RD18222>.
- Pan, Y., Kong, L.D., 2018. High fructose diet-induced metabolic syndrome: Pathophysiological mechanism and treatment by traditional Chinese medicine. *Pharmacol. Res.* <https://doi.org/10.1016/j.phrs.2018.02.020>.
- Pham, C.V., Pham, T.T., Lai, T.T., Trinh, D.C., Nguyen, H.V.M., Ha, T.T.M., Phuong, T.T., Tran, L.D., Winkler, C., To, T.T., 2019. Icaritin reduces bone loss in a Rankl-induced transgenic medaka (*Oryzias latipes*) model for osteoporosis. *J. Fish Biol.* <https://doi.org/10.1111/jfb.14241>.
- Pu, P., Gao, D.M., Mohamed, S., Chen, J., Zhang, J., Zhou, X.Y., Zhou, N.J., Xie, J., Jiang, H., 2012. Naringin ameliorates metabolic syndrome by activating AMP-activated protein kinase in mice fed a high-fat diet. *Arch. Biochem. Biophys.* 518, 61–70. <https://doi.org/10.1016/j.abb.2011.11.026>.
- Qi, M.Y., Kai-Chen, Liu, H.R., Su, Y.H., Yu, S.Q., 2011. Protective effect of Icaritin on the early stage of experimental diabetic nephropathy induced by streptozotocin via modulating transforming growth factor  $\beta$  1 and type IV collagen expression in rats. *J. Ethnopharmacol.* 138, 731–736. <https://doi.org/10.1016/j.jep.2011.10.015>.
- Qi, S., He, J., Zheng, H., Chen, C., Lan, S., 2019. Icaritin prevents diabetes-induced bone loss in rats by reducing blood glucose and suppressing bone turnover. *Molecules* 24. <https://doi.org/10.3390/molecules24101871>.
- Qiao, C., Wang, H., Song, Z., Ding, Y., Tao, J., Ai, J., Ding, X., 2020. Icaritin Attenuates Diabetic Cardiomyopathy and Downregulates Extracellular Matrix Proteins in Heart Tissue of Type 2 Diabetic Rats. *Pharmacology*. <https://doi.org/10.1159/000505408>.
- Reddy, P., Lent-Schochet, D., Ramakrishnan, N., McLaughlin, M., Jialal, I., 2019. Metabolic syndrome is an inflammatory disorder: A conspiracy between adipose tissue and phagocytes. *Clin. Chim. Acta.* <https://doi.org/10.1016/j.cca.2019.06.019>.
- Ruderman, N.B., Carling, D., Prentki, M., Cacicedo, J.M., 2013. AMPK, insulin resistance, and the metabolic syndrome. *J. Clin. Invest.* <https://doi.org/10.1172/JCI67227>.
- Saklayen, M.G., 2018. The Global Epidemic of the Metabolic Syndrome. *Curr. Hypertens. Rep.* <https://doi.org/10.1007/s11906-018-0812-z>.
- Salminen, A., Hyttinen, J.M.T., Kaarniranta, K., 2011. AMP-activated protein kinase inhibits NF- $\kappa$ B signaling and inflammation: Impact on healthspan and lifespan. *J. Mol. Med.* <https://doi.org/10.1007/s00109-011-0748-0>.
- Shackelford, D.B., Shaw, R.J., 2009. The LKB1-AMPK pathway: Metabolism and growth control in tumour suppression. *Nat. Rev. Cancer.* <https://doi.org/10.1038/nrc2676>.
- Shao-Rui, C., Xiang-Zhen, X., Yu-Hua, W., Jian-Wen, C., Suo-Wen, X., Lian-Quan, G., Pei-Qing, L., 2010. Icaritin derivative inhibits inflammation through suppression of p38 mitogen-activated protein kinase and nuclear factor- $\kappa$ B pathways. *Biol. Pharm. Bull.* 33, 1307–1313. <https://doi.org/10.1248/bpb.33.1307>.
- Sharma, H., Kumar, S., 2016. Natural AMPK Activators: An Alternative Approach for the Treatment and Management of Metabolic Syndrome. *Curr. Med. Chem.* 24, 1007–1047. <https://doi.org/10.2174/0929867323666160406120814>.
- Sharma, P., 2011. Inflammation and the metabolic syndrome. *Indian J. Clin. Biochem.* <https://doi.org/10.1007/s12291-011-0175-6>.
- Sherling, D.H., Perumareddi, P., Hennekens, C.H., 2017. Metabolic Syndrome: Clinical and Policy Implications of the New Silent Killer. *J. Cardiovasc. Pharmacol. Ther.* <https://doi.org/10.1177/1074248416686187>.
- Srikanthan, K., Feyh, A., Visweshwar, H., Shapiro, J.L., Sodhi, K., 2016. Systematic review of metabolic syndrome biomarkers: A panel for early detection, management, and risk stratification in the West Virginian population. *Int. J. Med. Sci.* <https://doi.org/10.7150/ijms.13800>.
- Tappy, L., 2018. Fructose-containing caloric sweeteners as a cause of obesity and metabolic disorders. *J. Exp. Biol.* <https://doi.org/10.1242/jeb.164202>.
- Wang, X., Liu, Chuanhai, Xu, Yong, Chen, P., Shen, Y., Xu, Yansheng, Zhao, Y., Chen, W., Zhang, X., Ouyang, Y., Wang, Y., Xie, C., Zhou, M., Liu, Cuihong, 2017. Combination of mesenchymal stem cell injection with icaritin for the treatment of diabetes-associated erectile dysfunction. *PLoS ONE* 12, 1–18. <https://doi.org/10.1371/journal.pone.0174145>.
- Wang, Y.M., Zhang, B., Xue, Y., Li, Z.J., Wang, J.F., Xue, C.H., Yanagita, T., 2010. The mechanism of dietary cholesterol effects on lipids metabolism in rats. *Lipids Health Dis.* 9. <https://doi.org/10.1186/1476-511X-9-4>.
- Xin, H., Zhou, F., Liu, T., Li, G.Y., Liu, J., Gao, Z.Z., Bai, G.Y., Lu, H., Xin, Z.C., 2012. Icaritin ameliorates streptozotocin-induced diabetic retinopathy in Vitro and in Vivo. *Int. J. Mol. Sci.* 13, 866–878. <https://doi.org/10.3390/ijms13010866>.
- Xu, F., Ding, Y., Guo, Y., Liu, B., Kou, Z., Xiao, W., Zhu, J., 2016. Anti-osteoporosis effect of Epimedium via an estrogen-like mechanism based on a system-level approach. *J. Ethnopharmacol.* 177, 148–160. <https://doi.org/10.1016/j.jep.2015.11.007>.
- Yang, X.H., Li, L., Xue, Y.B., Zhou, X.X., Tang, J.H., 2020. Flavonoids from Epimedium pubescens: Extraction and mechanism, antioxidant capacity and effects on CAT and GSH-Px of *Drosophila melanogaster*. *PeerJ* 2020. <https://doi.org/10.7717/peerj.8361>.
- Yunk-yung, H.A.N., Mi-young, S., Min-sub, H., Ji-hye, H., Yong-ki, P., Hyo-won, J., 2016. Epimedium koreanum Nakai and its main constituent icaritin suppress lipid accumulation during adipocyte differentiation of 3T3-L1 preadipocytes. *Chin. J. Nat. Med.* 14, 671–676. [https://doi.org/10.1016/S1875-5364\(16\)30079-6](https://doi.org/10.1016/S1875-5364(16)30079-6).
- Zhang, W.P., Bai, X.J., Zheng, X.P., Xie, X.L., Yuan, Z.Y., 2013. Icaritin attenuates the enhanced prothrombotic state in atherosclerotic rabbits independently of its lipid-lowering effects. *Planta Med.* 79, 731–736. <https://doi.org/10.1055/s-0032-1328551>.
- Zheng, J., Ramirez, V.D., 2000. Inhibition of mitochondrial proton F0F1-ATPase/ATP synthase by polyphenolic phytochemicals. *Br. J. Pharmacol.* 130, 1115–1123. <https://doi.org/10.1038/sj.bjp.0703397>.
- Zheng, Z.G., Zhou, Y.P., Zhang, X., Thu, P.M., Xie, Z.S., Lu, C., Pang, T., Xue, B., Xu, D.Q., Chen, Y., Chen, X.W., Li, H.J., Xu, X., 2016. Anhydroicaritin improves diet-induced obesity and hyperlipidemia and alleviates insulin resistance by suppressing SREBPs activation. *Biochem. Pharmacol.* 122, 42–61. <https://doi.org/10.1016/j.bcp.2016.10.016>.